Molecular Crystals and Liquid Crystals
Publication details, including instructions for authors and subscription information:
http://www.informaworld.com/smpp/title~content=t713644168

Synthesis and Mesomorphic Properties of 6-Methoxy- and 6-Ethoxy-2-(2-Hydroxy-4-Alkanoyloxybenzylidenamino)Benzothiazoles

Sie-Tiong Ha[a]; Teck-Ming Koh[b]; Guan-Yeow Yeap[c]; Hong-Cheu Lin[d]; Siew-Ling Lee[e]; Yip-Foo Win[a]; Siew-Teng Ong[a]
[a] Department of Chemical Science, Faculty of Science, University Tunku Abdul Rahman, Jln University, Bandar Barat, Kampar, Perak, Malaysia [b] Department of Science, Faculty of Engineering & Science, University Tunku Abdul Rahman, Jln Genting Kelang, Setapak, Kuala Lumpur, Malaysia [c] Liquid Crystal Research Laboratory, School of Chemical Sciences, University Sains Malaysia, Minden, Penang, Malaysia [d] Department of Materials Science & Engineering, National Chiao Tung University, Hsinchu, Taiwan, Republic of China [e] Ibnu Sina Institute for Fundamental Science Studies, University Teknologi Malaysia, Skudai, Johor, Malaysia

First published on: 20 October 2010

To cite this Article Ha, Sie-Tiong , Koh, Teck-Ming , Yeap, Guan-Yeow , Lin, Hong-Cheu , Lee, Siew-Ling , Win, Yip-Foo and Ong, Siew-Teng(2010) 'Synthesis and Mesomorphic Properties of 6-Methoxy- and 6-Ethoxy-2-(2-Hydroxy-4-Alkanoyloxybenzylidenamino)Benzothiazoles', Molecular Crystals and Liquid Crystals, 528: 1, 10 — 22
To link to this Article: DOI: 10.1080/15421406.2010.504510
URL: http://dx.doi.org/10.1080/15421406.2010.504510

Mol. Cryst. Liq. Cryst., Vol. 528: pp. 10–22, 2010

ISSN: 1542-1406 print/1563-5287 online
DOI: 10.1080/15421406.2010.504510

Taylor & Francis
Taylor & Francis Group

Synthesis and Mesomorphic Properties of 6-Methoxy- and 6-Ethoxy-2-(2-Hydroxy-4-Alkanoyloxybenzylidenamino)Benzothiazoles

SIE-TIONG HA,[1] TECK-MING KOH,[2] GUAN-YEOW YEAP,[3] HONG-CHEU LIN,[4] SIEW-LING LEE,[5] YIP-FOO WIN,[1] AND SIEW-TENG ONG[1]

[1]Department of Chemical Science, Faculty of Science, University Tunku Abdul Rahman, Jln University, Bandar Barat, Kampar, Perak, Malaysia
[2]Department of Science, Faculty of Engineering & Science, University Tunku Abdul Rahman, Jln Genting Kelang, Setapak, Kuala Lumpur, Malaysia
[3]Liquid Crystal Research Laboratory, School of Chemical Sciences, University Sains Malaysia, Minden, Penang, Malaysia
[4]Department of Materials Science & Engineering, National Chiao Tung University, Hsinchu, Taiwan, Republic of China
[5]Ibnu Sina Institute for Fundamental Science Studies, University Teknologi Malaysia, Skudai, Johor, Malaysia

Two new series of Schiff base thermotropic liquid crystals, 6-methoxy-2-(2-hydroxy-4-alkanoyloxybenzylidenamino)benzothiazoles and 6-ethoxy-2-(2-hydroxy-4-alkanoyloxybenzylidenamino)benzothiazoles, comprising different terminal groups, a methoxyl and ethoxyl group, respectively, were synthesized. Structural elucidation was carried out using elemental analysis and spectroscopic techniques such as Fourier transform infrared (FTIR), ^{1}H and ^{13}C nuclear magnetic resources (NMR), and mass spectrometry. The mesomorphic properties and thermal stabilities of the title compounds were studied by using differential scanning calorimetry, optical polarizing microscopy, and thermogravimetric analysis. No liquid-crystal phases were observed for the short-chain members ($n = 2$ and 3) in both series, and the remaining members all exhibited nematic phase with Schlieren or marble-like textures. Effects of the lateral hydroxyl group, terminal group, and the length of the terminal alkanoyloxy chain on the mesomorphic properties are discussed. Structure-property relationships were established upon comparison with other structurally related compounds.

Keywords Benzothiazole liquid crystals; lateral hydroxyl group; nematic; structure-property relationship; terminal group

Address correspondence to Sie-Tiong Ha, Department of Chemical Science, Faculty of Science, University Tunku Abdul Rahman, Jln University, Bandar Barat, 31900 Kampar, Perak, Kuala Lumpur 53300, Malaysia. E-mail: hast@utar.edu.my

Introduction

Since the 1960s, the unique properties of liquid crystals have been extensively applied in modern technology such as liquid-crystal displays (LCDs), thermocromic materials, and many other areas. In general, rod-like (calamitic) molecules are highly favorable in inducing mesomorphic behavior due to their high shape anisotropy [1–3]. A mesogenic core, terminal groups, and a flexible terminal chain are the fundamental prerequisites in designing new thermotropic liquid crystals [4].

It is also commonly believed that molecular order in liquid-crystal phases depends largely on the structure of the mesogenic core: its geometry, polarizability, molecular conformation, length-to-breath ratio, as well as the number and position of permanent dipole moments [5]. Mesogenic compounds having single-ring heterocyclic moieties, such as pyridine [6], thiophene [7] and 1,3,4-thiadiazole [8], have been reported in the literature. These heterocyclic mesogens are usually incorporated with heteroatoms, such as N, O, and S, resulting in a reduced symmetry in the overall molecule together with a stronger polar induction. The inclusion of the heteroatoms can significantly change the polarity, polarizability, and, to a certain extent, geometry of a molecule, thereby influencing its type of mesophase, the phase transition temperatures, dielectric constants, and other properties [9,10].

Benzothiazole derivatives, an important class of heterocyclic compounds, have been extensively studied due to their potent antitumor and antibacterial activities [11]. Benzothiazole-type liquid crystals have been proven to exhibit good hole-transporting properties with a low ionization potential, making them potential hole-transporting materials in organic light-emitting devices (OLEDs) [12]. However, examples of benzothiazole-based liquid crystals are relatively scant. Pavluchenko *et al.* [13] reported on mesogens comprising benzothiazole and benzoxazole moieties with different central linkages and lateral substituents at different positions to evaluate the effect of structural changes on mesomorphic properties. Additionally, benzothiazole-type mesogens having an azo central linkage with different terminal groups (OCH_3, Cl, and NO_2) at the sixth position of the benzothiazole moiety have been reported recently [14–16] in which the nitro substituent was found to be more conducive to the generation of the smectic mesophase compared to the chloro and methoxyl substituents.

Furthermore, it was believed that the lateral hydroxyl group could have disrupted or even destroyed mesomorphism due to strong intermolecular hydrogen bonding [17]. However, previous study has shown that the presence of the lateral hydroxyl group at the *ortho*-position may have led to an increase in the molecular polarizability as well as in the clearing temperature [18]. The lateral hydroxyl group, on the other hand, can also enhance the stability of a molecule through intramolucular hydrogen bonding [19].

As a continuation of our previous work on the synthesis and study of mesomorphic properties of compounds bearing a benzothiazole core unit, here we have synthesized two new mesogenic homologous series of benzothiazole derivatives, each having a Schiff base central linkage, a lateral hydroxyl group, and different terminal groups (OCH_3 and OC_2H_5).

Experimental

4-Dimethylaminopyridine (DMAP) and fatty acids ($C_{n-1}H_{2n-1}COOH$ where $n = 2$, 4, 6, 7, 12, 14, 16, 18) were obtained from Merck (Darmstadt, Germany).

2-Amino-6-ethoxybenzothiazole, 2-amino-6-methoxybenzothiazole, 2,4-dihydroxybenzaldehyde, fatty acids ($C_{n-1}H_{2n-1}COOH$ where $n = 3$, 5, 8, 10), and *N*,*N*′-dicyclohexylcarbodiimide (DCC) were purchased from Acros Organics (New Jersey, USA). All solvents and reagents were purchased commercially and used without any further purification.

Fourier transform infrared (FTIR) analyses were performed on a Perkin-Elmer System 2000 FTIR Spectrometer (Universiti Tunku Abdul Rahman and Universiti Sains Malaysia). All compounds were analyzed using KBr discs with a measurement range from 4000 to 400 cm^{-1}. The ^1H nuclear magnetic resonance (NMR) (400 MHz) and ^{13}C NMR (100 MHz) spectra were recorded in $CDCl_3$ using a JEOL LA-400 MHz NMR spectrometer with tetramethylsilane (TMS) as the internal standard. Electron ionization mass spectrometry (EI-MS) (70 eV) were measured with a Finnigan MAT95XL-T mass spectrometer at a source temperature of 200°C. Microanalyses were carried out on Perkin Elmer 2400 LS Series CHNS/O analyzer. Thin-layer Chromatography (TLC) was carried out on aluminum-backed silica-gel plates (Merck 60 F_{254} (Darmstadt, Germany)) and visualized under short-wave ultraviolet (UV) light.

Phase-transition temperatures and enthalpy changes were measured using a Mettler Toledo DSC823^e differential scanning calorimeter at heating and cooling rates of 10°C/min and −10°C/min, respectively. Thermogravimetric analysis was performed on a Mettler Toledo thermal gravimetric Analyzer, which consisted of a TGA/SDTA851^e main unit and a STARe software at a heating rate of 20°C/min in nitrogen atmosphere. A polarizing optical microscope (Carl Zeiss, Universiti Sains Malaysia) equipped with a Linkam heating stage was used for temperature dependent studies of the liquid-crystal textures. A video camera (Video Master coomo20P) installed on the polarizing microscope was coupled to a video capture card (Video Master coomo600), allowing real-time video capture and image saving. The textures exhibited by the compounds were observed using polarized light with crossed polarizers. Samples were prepared as thin films sandwiched between a glass slide and a coverslip.

Synthesis

12MHBABTH. The synthetic route for the title compounds is depicted in Scheme 1. 2-Amino-6-methoxybenzothiazole (40 mmol, 7.21 g) and 2,4-dihydroxybenzaldehyde (40 mmol, 5.52 g) were dissolved in 60 mL ethanol. Two drops of acetic acid were added and the mixture was refluxed for 3 h upon stirring. The mixture was then filtered and the filtrate was left to evaporate to dryness. The yellow solid that was formed was recrystallized with ethanol for further reaction. The benzothiazole intermediate **1** (20 mmol), along with the appropriate fatty acid (20 mmol) and DMAP (4 mmol, 0.49 g) were dissolved in a 50-mL mixture of dichloromethane (DCM) and dimethylformamide (DMF) and stirred at 0°C. DCC (20 mmol, 4.13 g) dissolved in 10 ml of DCM was added into the mixture dropwise and continuously stirred for an hour at 0°C. The mixture was then stirred at room temperature for another 3 h. Finally, the mixture was filtered and the solvent was removed by evaporation. The yellow solid obtained was recrystallized using ethanol. Infrared (IR) (KBr) ν_{max} cm^{-1} 3431 (O−H), 3069 (C−H aromatic), 2921, 2851 (C−H aliphatic), 1758 (C=O ester), 1611 (C=N thiazole). ^1H NMR (400 MHz, $CDCl_3$): δ/ppm 0.9 (t, $J = 6.6$ Hz, 3H, $C\underline{H}_3-$), 1.2–1.4 (m, 16H, $CH_3(C\underline{H}_2)_8-$), 1.8 (q, $J = 7.3$ Hz, 2H, $-C\underline{H}_2CH_2COO-$), 2.6 (t, $J = 7.3$ Hz, 2H, $-C\underline{H}_2\overline{C}OO-$), 3.9 (s, 3H, $C\underline{H}_3O-$), 6.7 (d, $J = 8.5$ Hz, 1H, Ar-H), 6.8 (s, 1H,

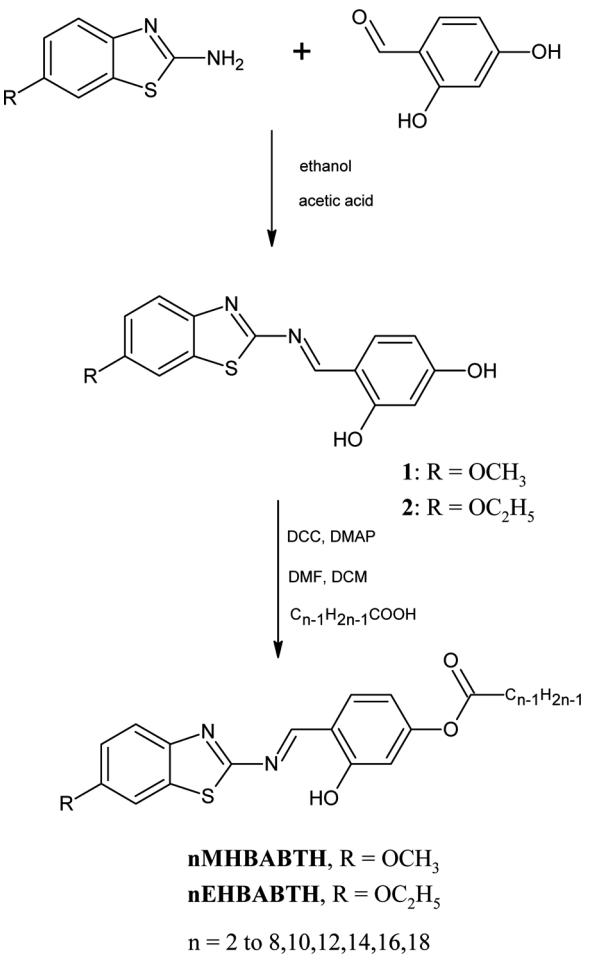

Scheme 1. Synthetic route of **nMHBABTH** and **nEHBABTH**.

Ar-H), 7.1 (d, $J = 9.0$ Hz, 1H, Ar-H), 7.2 (s, 1H, Ar-H), 7.5 (d, $J = 8.5$ Hz, 1H, Ar-H), 7.8 (d, $J = 8.8$ Hz, 1H, Ar-H), 9.2 (s, 1H, −N=CH−), 12.5 (s, 1H, OH). ^{13}C NMR (400 MHz, $CDCl_3$): δ/ppm 171.54 (−COO−), 166.45 (C=N), 165.36, 163.20, 157.88, 156.15, 145.90, 136.02, 134.88, 123.76, 116.41, 116.12, 113.87, 110.76, 104.42 for aromatic carbons, 55.86 (CH_3O−), 34.53 (−CH_2COO−), 32.01 (−CH_2CH_2COO−), 29.70, 29.55, 29.43, 29.35, 29.15, 24.93, 22.78 for methylene carbons [$CH_3(CH_2)_{12}CH_2CH_2$COO−], 14.23 [$CH_3(CH_2)_{14}$COO−]. EI-MS m/z (rel. int. %): 482 (9) [M^+], 300 (100).

16EHBABTH. The synthetic method is identical to that of **12MHBABTH**. IR (KBr) ν_{max} cm^{-1} 3420 (O−H), 3075 (C−H aromatic), 2922, 2850 (C−H aliphatic), 1758 (C=O ester), 1609 (C=N, thiazole). ^{1}H NMR (400 MHz, $CDCl_3$): δ/ppm 0.9 (t, $J = 6.6$ Hz, 3H, CH_3−), 1.2 (m, 24H, $CH_3(CH_2)_{12}CH_2CH_2$COO−), 1.5 (t, $J = 7.2$ Hz, 3H, CH_3CH_2O−), 1.8 (q, $J = 7.1$ Hz, 2H, −CH_2CH_2COO−), 2.6 (t, $J = 7.4$ Hz, 2H, −CH_2COO−), 4.1 (q, $J = 6.9$ Hz, 2H, CH_3CH_2O−), 6.7 (d, $J = 8.5$ Hz, 1H, Ar-H), 6.8 (s, 1H, Ar-H), 7.1 (d, $J = 8.8$ Hz, 1H, Ar-H), 7.3 (s, 1H,

Ar-H), 7.5 (d, $J = 8.5$ Hz, 1H, Ar-H), 7.8 (d, $J = 9.1$ Hz, 1H, Ar-H), 9.2 (s, 1H, −N=CH−), 12.5 (s, 1H, OH). ^{13}C NMR (400 MHz, $CDCl_3$): δ/ppm 171.40 (−COO−), 166.24 (C=N), 165.18, 163.07, 157.15, 156.02, 145.70, 135.89, 134.74, 123.63, 116.42, 116.31, 113.74, 110.63, 104.96 for aromatic carbons, 64.08 (CH_3CH_2O−), 34.41, 31.90, 29.68, 29.64, 29.57, 29.42, 29.34, 29.22, 29.04, 24.82, 22.67 for methylene carbons [$CH_3(CH_2)_{14}COO$−], 14.78 (CH_3CH_2O−), 14.10 [$CH_3(CH_2)_{14}COO$−]. EI-MS m/z (rel. int. %): 552(15) $(M)^+$, 312 (100).

Results and Discussion

Structural identification of the title compounds was carried out by employing a combination of elemental analysis and spectroscopic techniques (FTIR, NMR, and EI-MS). The percentages of C, H, and N from the elemental analysis (Tables 1 and 2) conform with the calculated values for compounds **nMHBABTH** and **nEHBABTH**. The prominent molecular ion peaks in the mass spectra of **12MHBABTH** and **16EHBABTH** at m/z 482 and 552, respectively, established a molecular formula of $C_{27}H_{34}N_2O_4S$ and $C_{32}H_{44}N_2O_4S$, thus supporting the proposed structures.

Mesomorphic Behavior and Thermogravimetric Analysis

All the title compounds were investigated by polarizing optical microscopy (POM) and differential scanning calorimetry (DSC) to determine their mesomorphic properties. Phase transition temperatures and corresponding enthalpy changes of compound **nMHBABTH** and **nEHBABTH** were determined using DSC. The data for **nMHBABTH** and **nEHBABTH** obtained from the DSC analysis are tabulated in Tables 3 and 4, respectively. The short-chain members ($n = 2$, 3, and 4) of **nMHBABTH** and all members of **nEHBABTH** exhibited no distinct exothermic peaks during the cooling cycle due to the partial decomposition of the compounds. This phenomenon was also observed in the work of Wei *et al.* [20]. The decomposition temperatures were further confirmed by thermogravimetric analysis (TGA;

Table 1. Percentage yields and analytical data of **nMHBABTH**

Compound	Yield (%)	% Found (% Calcd.)			
		Formula	C	H	N
2MHBABTH	26	$C_{17}H_{14}N_2O_4S$	59.72 (59.64)	4.01 (4.12)	8.05 (8.18)
3MHBABTH	21	$C_{18}H_{16}N_2O_4S$	60.78 (60.66)	4.48 (4.53)	7.79 (7.86)
4MHBABTH	32	$C_{19}H_{18}N_2O_4S$	61.69 (61.61)	4.83 (4.90)	7.50 (7.56)
5MHBABTH	36	$C_{20}H_{20}N_2O_4S$	62.43 (62.48)	5.27 (5.24)	7.37 (7.29)
6MHBABTH	40	$C_{21}H_{22}N_2O_4S$	63.41 (63.30)	5.50 (5.56)	6.94 (7.03)
7MHBABTH	48	$C_{22}H_{24}N_2O_4S$	64.16 (64.06)	5.80 (5.86)	6.71 (6.79)
8MHBABTH	41	$C_{23}H_{26}N_2O_4S$	64.83 (64.77)	6.10 (6.14)	6.47 (6.57)
10MHBABTH	55	$C_{25}H_{30}N_2O_4S$	66.11 (66.05)	6.57 (6.65)	6.12 (6.16)
12MHBABTH	46	$C_{27}H_{34}N_2O_4S$	67.07 (67.19)	7.16 (7.10)	5.75 (5.80)
14MHBABTH	59	$C_{29}H_{38}N_2O_4S$	68.27 (68.20)	7.48 (7.50)	5.47 (5.49)
16MHBABTH	63	$C_{31}H_{42}N_2O_4S$	69.19 (69.11)	7.79 (7.86)	5.22 (5.20)
18MHBABTH	67	$C_{33}H_{46}N_2O_4S$	69.99 (69.93)	8.10 (8.18)	4.91 (4.94)

Table 2. Percentage yields and analytical data of **nEHBABTH**

Compound	Yield (%)	% Found (% Calcd.)			
		Formula	C	H	N
2EHBABTH	23	$C_{18}H_{16}N_2O_4S$	60.78 (60.66)	4.50 (4.53)	7.75 (7.86)
3EHBABTH	28	$C_{19}H_{18}N_2O_4S$	61.66 (61.61)	4.85 (4.90)	7.50 (7.56)
4EHBABTH	31	$C_{20}H_{20}N_2O_4S$	62.40 (62.48)	5.13 (5.24)	7.31 (7.29)
5EHBABTH	37	$C_{21}H_{22}N_2O_4S$	63.25 (63.30)	5.63 (5.56)	7.09 (7.03)
6EHBABTH	35	$C_{22}H_{24}N_2O_4S$	64.00 (64.06)	5.90 (5.86)	6.82 (6.79)
7EHBABTH	36	$C_{23}H_{26}N_2O_4S$	64.69 (64.77)	6.21 (6.14)	6.59 (6.57)
8EHBABTH	42	$C_{24}H_{28}N_2O_4S$	65.47 (65.43)	6.30 (6.41)	6.66 (6.63)
10EHBABTH	40	$C_{26}H_{32}N_2O_4S$	66.72 (66.64)	6.79 (6.88)	5.90 (5.98)
12EHBABTH	55	$C_{28}H_{36}N_2O_4S$	67.76 (67.71)	7.24 (7.31)	5.67 (5.64)
14EHBABTH	58	$C_{30}H_{40}N_2O_4S$	68.61 (68.67)	7.66 (7.68)	5.31 (5.34)
16EHBABTH	61	$C_{32}H_{44}N_2O_4S$	69.62 (69.53)	7.98 (8.02)	5.02 (5.07)
18EHBABTH	65	$C_{34}H_{48}N_2O_4S$	70.39 (70.31)	8.24 (8.33)	4.85 (4.82)

Table 3. Transition temperatures and associated enthalpy changes of **nMHBABTH** upon heating

Compounds	Transition temperature (°C) (associated enthalpy changes, kJ mol^{-1})
2MHBABTH[a]	Cr 186.8 (45.57) I
3MHBABTH[a]	Cr 143.0 (35.55) I
4MHBABTH[a]	Cr 154.1 (36.58) N 162.4 (0.60) I
5MHBABTH	Cr 137.8 (33.89) N 147.6 (0.32) I
	Cr 92.8 (26.86) N 138.2 (0.33) I
6MHBABTH	Cr 131.1 (38.74) N 155.6 (0.63) I
	Cr 91.8 (32.89) N 141.8 (0.81) I
7MHBABTH	Cr_1 121.6 (1.13) Cr_2 133.6 (38.63) N 145.8 (0.49) I
	Cr 114.3 (40.13) N 143.6 (0.39) I
8MHBABTH	Cr 133.2 (37.66) N 145.8 (0.60) I
	Cr 100.7 (33.72) N 132.5 (0.84) I
10MHBABTH	Cr 127.5 (90.04) N 139.8 (1.81) I
	Cr 98.9 (89.07) N 135.9 (2.55) I
12MHBABTH	Cr 124.9 (43.25) N 136.8 (0.98) I
	Cr 107.7 (43.28) N 133.8 (0.53) I
14MHBABTH	Cr 123.6 (54.67) N 133.6 (0.84) I
	Cr 103.7 (53.75) N 130.7 (0.88) I
16MHBABTH	Cr 123.2 (61.86) N 129.7 (1.51) I
	Cr 95.7 (61.22) N 126.5 (1.51) I
18MHBABTH	Cr 122.3 (61.27) N 125.2 (1.23) I
	Cr 110.8 (58.31) N 117.0 (0.89) I

Cr = Crystal; N = nematic; I = isotropic liquid.

[a]Only heating data are provided. No distinct peak was detected during the cooling scan due to partial decomposition.

Cooling data was shown in italics.

Table 4. Transition temperatures and associated enthalpy changes of **nEHBABTH** upon heating

Compounds	Transition temperature (°C) (associated enthalpy changes, kJ mol^{-1})
2EHBABTH[a]	Cr 173.8 (50.4) I
3EHBABTH[a]	Cr 154.2 (54.9) I
4EHBABTH[a]	Cr 136.0 (33.9) N 175.9 (0.7) I
5EHBABTH[a]	Cr_1 80.6 (10.7) Cr_2 128.7 (34.0) N 162.1 (0.7) I
6EHBABTH[a]	Cr 128.6 (40.8) N 147.9 (0.7) I
7EHBABTH[a]	Cr 118.5 (38.5) N 155.1 (1.0) I
8EHBABTH[a]	Cr 128.6 (38.2) N 152.0 (0.8) I
10EHBABTH[a]	Cr 126.8 (47.5) N 149.0 (0.9) I
12EHBABTH[a]	Cr 126.5 (52.0) N 137.6 (1.1) I
14EHBABTH[a]	Cr 124.4 (49.7) N 129.5[b] I
16EHBABTH[a]	Cr 124.0 (59.7) N 130.0[b] I
18EHBABTH[a]	Cr 124.4 (73.0) N 127.9[b] I

Cr = Crystal; N = nematic; I = isotropic liquid.

[a]Only heating data are provided. No distinct peak was detected during the cooling scan due to its partial decomposition.

[b]POM data were used. The N-I transition was untraced by DSC analysis although this transition was observed through microscope studies.

Fig. 1). For instance, the decomposition temperature of **4MHBABTH** was found to be 168.38°C and the melting temperature from the DSC analysis was 162.4°C. A similar situation was observed for **6EHBABTH**.

From Tables 3 and 4 it is obvious that the ethanoyloxy and propanoyloxy derivatives are nonmesogenic compounds and the liquid-crystal phase only started to emerge from the butanoyloxy derivative onwards in both series. Observation under polarizing optical microscopy revealed that all the compounds are pure nematogens. Representative optical photomicrographs of **6MHBABTH** are depicted in Fig. 2. Upon cooling of **6MHBABTH** from its isotropic liquid phase, nematic droplets (Fig. 2a) appeared and coalesced with each other to form the classical nematic phase with a marbled-like texture (Fig. 2b). For series **nEHBABTH**, the representative optical photomicrographs of **10EHBABTH** are given in Fig. 3. Similarly, upon cooling of its isotropic liquid, the nematic phase was the first to emerge as small droplets (Fig. 3a) and, upon further cooling, nematic phase with disclination lines was formed (Fig. 3b). All observed liquid-crystalline textures are typical according to the literature [21,22].

The effects of the terminal alkanoyloxy chain on mesomorphic properties can be established by plotting a graph of phase transition temperature against the number of carbon atoms in the alkanoyloxy chain. According to Fig. 4, the odd–even effect was noticed in the short-chain members ($n = 4$, 5, 6, 7, and 8). In addition, the clearing temperatures of **nMHBABTH** exhibited a typical descending trend as the length of the carbon chain increased. This was attributed to the dilution of the mesogenic core, affected by the increase in the flexibility of the terminal alkanoyloxy chain [23]. This trend was in agreement with those homologous series of 2-(4-*n*-alkoxyphenylazo)-6-methoxybenzothiazoles reported by Prajapati and Bonde [16].

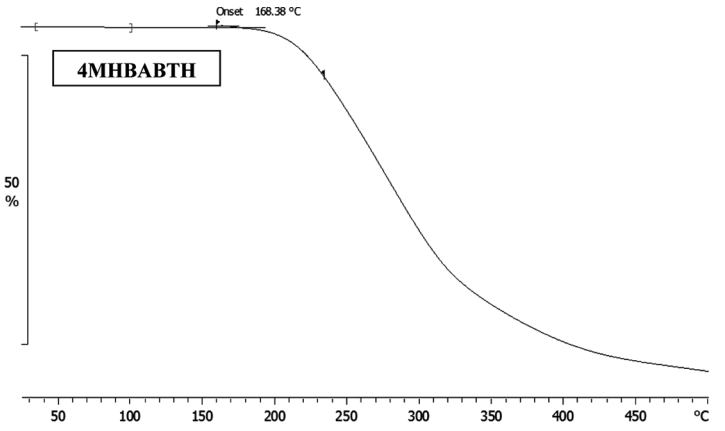

(a)

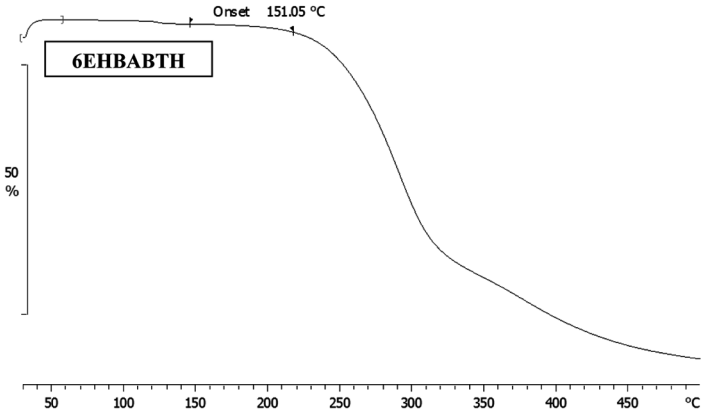

(b)

Figure 1. Thermogravimetric analysis curves of (a) **4MHBABTH** and (b) **6EHBABTH**.

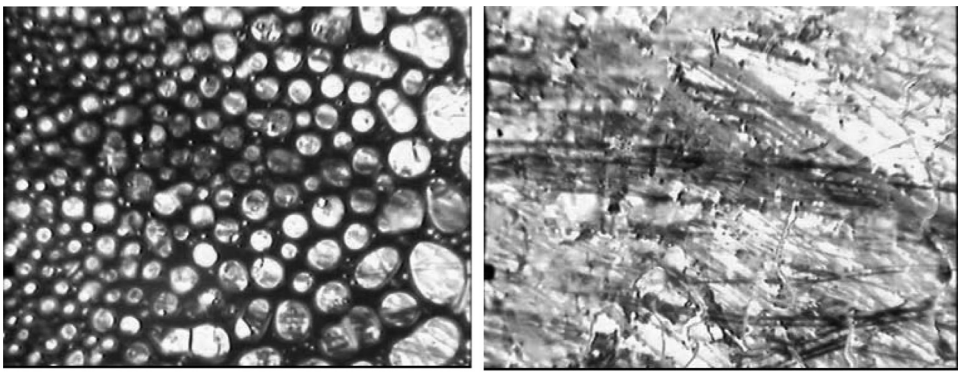

(a) (b)

Figure 2. Optical photomicrographs of **6MHBABTH**. Upon cooling from isotropic liquid, nematic droplets (a) appeared at 141°C and (b) coalesced to form the classical marble-like texture of the nematic phase.

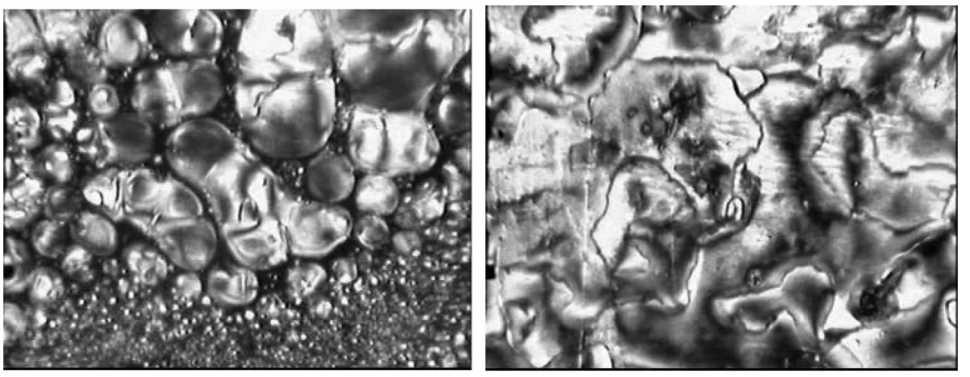

(a) (b)

Figure 3. Optical photomicrographs of **10EHBABTH**. During the first cooling under POM, the nematic phase emerged as small droplets (a) and coalesced with each other to form a Schlieren nematic phase with disclination lines (b).

Generally, short-chain members favor nematic formation, whereas the smectic phase is more favorable in long-chain members [5]. This general trend was obeyed by the **nMHBABTH** series depicted in Fig. 4 in which the nematic phase range reduced as the length of the terminal chain increased.

The plot of phase transition temperature against the number of carbon atoms in the terminal chain of **nEHBABTH** is depicted in Fig. 5. The odd–even effects on the mesomorphic properties are not that obvious but still observed for the C5 to C8 derivatives. The clearing temperatures showed a descending trend with the increase in the length of the carbon chain. Due to the same reason as discussed for series **nMHBABTH**, the nematic phase range was found to decrease as the length of the terminal alkyl chain is increased.

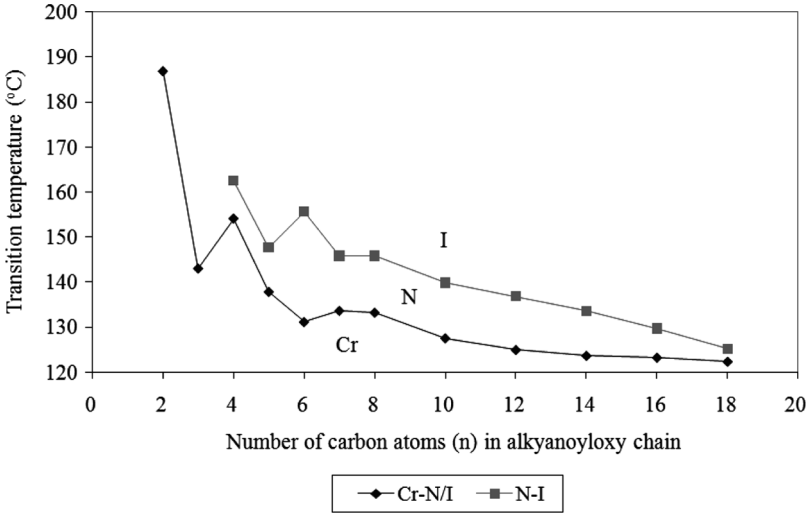

Figure 4. Plot of transition temperatures versus the number of carbons (n) in the alkanoyloxy chain of **nMHBABTH** during the heating cycle.

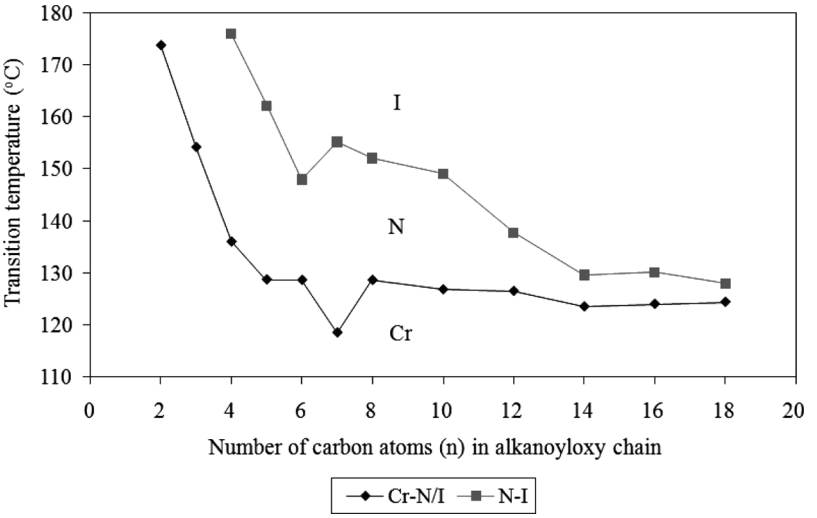

Figure 5. Plot of transition temperatures versus the number of carbons (n) in the alkanoyloxy chain of **nEHBABTH** during the heating cycle.

Chemical Structure-Mesomorphic Property Relationship

By comparing the present compounds to other structurally related compounds having different types of terminal groups, general rules for the effect of chemical constitution in nematogenic and smectogenic compounds can be deduced. In Table 5, the transition temperatures, types of mesophases, mesophase range, and molecular structures of **12MHBABTH** and **12EHBABTH** are compared with other structurally related compounds **A** [24], **B** [16], **C** [14], and **D** [15].

In order to clarify the importance of the terminal group on mesomorphic properties, we first compared **12MHBABTH** to compound **A**. Both compounds have a similar molecular structure, the only difference being in the terminal group, in which **12MHBABTH** possessed a terminal methoxyl group attached to the benzothiazole fragment unlike compound **A**. It can be noticed that **12MHBABTH** exhibited a nematic phase, whereas compound **A** is a non mesogenic compound. Therefore, the introduction of a polar group ($-OCH_3$) to **12MHBABTH** increased its polarizability, resulting in the emergence of a mesophase.

Comparison of the transition temperatures and the mesophase ranges between **12MHBABTH** and **12EHBABTH** revealed similarities. The similar polarities of the terminal methoxyl and ethoxyl groups resulted in both compounds exhibiting similar melting and clearing temperatures. An earlier report claimed that the terminal methoxyl group stabilizes the nematic phase, whereas the ethoxyl group or a longer alkoxyl chain at the sixth position of the benzothiazole ring will stabilize the smectic phase [25]. However, in the case of **12EHBABTH**, it exhibited a nematic phase instead. This is explained by the presence of the lateral hydroxyl group, which increased the broadness of the molecule, in turn facilitating the nematic phase instead of the smectic phase [5].

The main differences between **12MHBABTH** and compound **B** are in the linking group and the lateral substituent. **12MHBABTH** possesses a Schiff base linkage and a lateral hydroxyl group, and compound **B** consists of an azo linkage with an

Table 5. Transition temperatures, mesomorphic properties, and molecular structures of **12MHBABTH**, **12EHBABTH**, A, B, and C

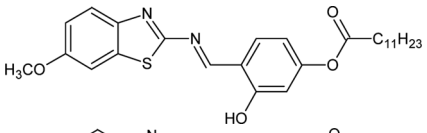

12MHBABTH

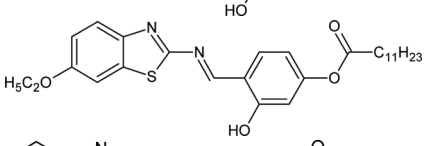

12EHBABTH

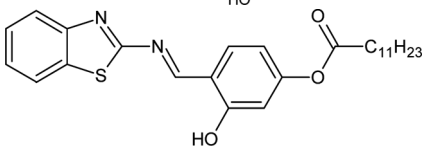

Compound A

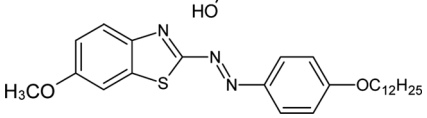

Compound B

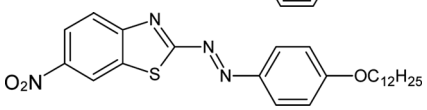

Compound C

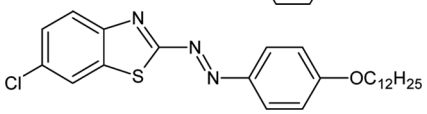

Compound D

Compound	Transition temperatures (°C)	Mesophase range (°C)		Commencement of smectic phase
		Sm	N	
12MHBABTH	Cr 124.9 N 136.8 I	—	11.9	—
12EHBABTH	Cr 126.5 N 137.6 I	—	11.1	—
A	Cr 99.9 I	—	—	—
B	Cr 113 (SmA 108)* N 135 I	—	22.0	C_{12}
C	Cr 156.0 SmA 194.0 I	38.0	—	C_4
D	Cr 80.0 SmA 172.0 I	90.0	—	C_5

*Means monotropic data.

absence of the lateral group. The melting temperature of **12MHBABTH** (124.9°C) was found to be higher than that of compound **B** (113°C), which could have been due to the intramolecular hydrogen bonding between the lateral hydroxyl (OH) and imine (CH=N) groups and the enhanced interactions arising from the overall geometry of the molecule [26]. However, the mesophase range of **12MHBABTH** (11.9°C) was smaller than that of compound **B** (22.0°C) resulting from the lateral hydroxyl group involved in a strong intermolecular hydrogen bonding (OH ···· N), leading to the disruption in the mesomorphism of the compound, hence depressing the mesophase range [17].

On the other hand, by incorporating more polar terminal groups (such as $-NO_2$ and $-Cl$) to compounds **C** and **D**, respectively, their mesophase ranges were found to

have increased dramatically to 38.0°C and 90°C. Moreover, another interesting behavior that was also observed for compounds **C** and **D** was that both exhibited an SmA phase instead of the nematic phase like in **12MHBABTH**. It might have been due to the presence of the polar group that favoured the lamellar packing, resulting in generation of the smectic phase.

Conclusions

Two nematic homologues series of 6-methoxy-2-(2-hydroxy-4-alkanoyloxybenzylidenamino)benzothiazoles and 6-ethoxy-2-(2-hydroxy-4-alkanoyloxybenzylidenamino)benzothiazoles were successfully synthesized and characterized. The short-chain derivatives ($n = 2$ and 3) were non-mesogenic compounds and the nematic phase was observed for the remaining members in both series. A polar terminal group is crucial in inducing mesophase formation. Although the lateral hydroxyl group increases the melting temperature due to intramolecular hydrogen bonding, it also decreases the mesophase range. More polar terminal groups such as nitro or chloro can be introduced to the compound in order to generate a smectic phase with a large mesophase range.

Acknowledgment

S. T. Ha is grateful to Universiti Tunku Abdul Rahman (UTAR) for the research facilities and financial support through the UTAR Research Fund (Vote No. 6200/H02). T. M. Koh acknowledges UTAR for the award of research and teaching assistantships.

References

[1] Imrie, C. T., & Henderson, P. A. (2002). *Cur. Op. Colloid. Inerface. Sci.*, *7*, 298–311.
[2] Yoshizawa, A., Kinbara, H., Narumi, T., Yamaguchi, A., & Dewa, H. (2005). *Liq. Cryst.*, *32*, 1175–1181.
[3] Imrie, C. T., & Luckhurst, G. R. (1998). *J. Mater. Chem.*, *8*, 1339–1343.
[4] Gray, G. W. (1987). *Thermotropic Liquid Crystals*, John Wiley, Chichester, England.
[5] Collings, P. J., & Hird, M. (1998). *Introduction to Liquid Crystals: Chemistry and Physics*. Taylor & Francis Ltd.: London, UK.
[6] Petrov, V. F., Pavluchenko, A. I., & Smirnova, N I. (1995). *Mol. Cryst. Liq. Cryst.*, *265*, 47–53.
[7] Parra, M., Belmar, J., Zunza, H., Zuniga, C., Villouta, S., & Martinez, R. (1993). *Bol. Soc. Chil. Quim.*, *38*, 325–330.
[8] Campbell, N. L., Duffy, W. L., Thomas, G. L., Wild, J. H., Kelly, S. M., Bartle, K., O'Neill, M., Minter, V., & Tuffin, R. P. (2002). *J. Mater. Chem.*, *12*, 2706–2721.
[9] Bartulin, J., Zuniga, C., Ramirez, A., Muller, H., Taylor, T. R. (1990). *Mol. Cryst. Liq. Cryst.*, *185*, 131–140.
[10] Karamysheva, L. A., Kovshev, E. L., Pavluchenko, A. I., Roitman, K. V., Titov, V. V., Torgova, S. I., & Grebenkin, M. F. (1981). *Mol. Cryst. Liq. Cryst.*, *67*, 241–251.
[11] (a) Racane, L., Stojkovic, R., Tralic-Kulenovic, V., & Karminski-Zamola, G. (2006). *Molecules*, *11*, 325–333; (b) Kini, S., Swain, S. P., & Gandhi, A. M. (2007). *Indian J. Pharmacent. Sci.*, *69*, 46–50; (c) Wells, G., Lowe, P. R., & Stevens, M. F. G. (2000). *Arkivoc.*, *1*, 779–797; (d) Chavan, A. A., & Pai, N. R. (2007). *Molecules*, *12*, 2467–2477.

[12] (a) Funahashi, M., & Hanna, J. I. (1996). *Jpn. J. Appl. Phys.*, *35*, L703–L705; (b) Funahashi, M., & Hanna, J. I. (1997). *Phys. Rev. Lett.*, *78*, 2184–2187; (c) Funahashi, M., & Hanna, J. I. (1997). *Mol. Cryst. Liq. Cryst.*, *304*, 429–434.
[13] Pavluchenko, A. I., Smirnova, N. I., Titov, V. V., Kovahev, E. I., & Djumaev, K. M. (1976). *Mol. Cryst. Liq. Cryst.*, *37*, 35–46.
[14] Prajapati, A. K., & Bonde, N. L. (2009). *Mol. Cryst. Liq. Cryst.*, *501*, 72–85.
[15] Prajapati, A. K., & Bonde, N. L. (2005). Mesogenic benzothiazole derivative, Proceedings of the 11th National Conference on Liquid Crystals, 1–3 November Allahabad, India.
[16] Prajapati, A. K., & Bonde, N. L. (2006). *J. Chem. Sci.*, *118*, 203–210.
[17] Gray, G. W. (1962). *Molecular Structure and Properties of Liquid Crystals*, Academic Press: London.
[18] Yeap, G. Y., Ha, S. T., Lim, P. L., Boey, P. L., & Mahmood, W. A. K. (2004). *Mol. Cryst. Liq. Cryst.*, *423*, 73–84.
[19] Hallsby, A., Nilsson, M., & Otterholm, B. (1982). *Mol. Cryst. Liq. Cryst.*, *82*, 61–68.
[20] Wei, Q., Shi, L., Cao, H., Wang, L. P., Yang, H., Wang, Y. B. (2008). *Liq. Cryst.*, *35*, 581–585.
[21] Demus, D., & Richter, L. (1978). *Textures of Liquid Crystals*, Verlag Chemie: New York.
[22] Dierking, I. (2003). *Textures of Liquid Crystals*, Wiley-VCH: Weinheim.
[23] Berdague, P., Bayle, J. P., Ho, M. S., & Fung, B. M. (1993). *Liq. Cryst.*, *14*, 667–674.
[24] Ha, S. T., Koh, T. M., Lin, H. C., Yeap, G. Y., Win, F. W., Ong, S. T., Sivasothy, Y., & Ong, L. K. (2009). *Liq. Cryst.*, *36*, 917–925.
[25] Ha, S. T., Koh, T. M., Yeap, G. Y., Lin, H. C., Boey, P. L., Win, Y. F., Ong, S. T., & Ong, L. K. (2009). *Mol. Cryst. Liq. Cryst.*, *506*, 56–70.
[26] Dixit, S., & Vora, R. A. (2009). *Mol. Cryst. Liq. Cryst.*, *501*, 43–52.